applied sciences

MDPI

Article

Research on Coal Seam Deformation Risk Based on In Situ Stress Evaluation and Numerical Simulation

Lei Feng [1], Fei Zhang [1], Yuan Hao [2], Baoan Xian [3,*], Yansen Bi [3] and Yongdong Fan [4]

[1] China United Coalbed Methane Corp., Ltd., Beijing 100015, China
[2] Wulumuqi Guosheng Huidong New Energy Co., Ltd., Wulumuqi 830063, China
[3] School of Resources and Environment, Polytechnic University, Jiaozuo 454003, China
[4] College of Petroleum Engineering, Xi'an Petroleum University, Xi'an 710065, China
* Correspondence: xba@hpu.edu.cn

Abstract

Coal seam casing deformation is a key engineering challenge restricting the efficient development of coalbed methane. Frequent casing deformation in complex tectonic stress zones seriously affects wellbore integrity and fracturing performance. This study takes the in situ stress characteristics of coal seams and the mechanism of casing deformation as the research objects, comprehensively employing theoretical analysis and numerical simulation methods to systematically carry out in situ stress evaluation, numerical simulation of casing deformation, and sensitivity analysis of formation dip angle. First, based on five indicators, including stress difference, stress ratio, maximum shear stress, lateral pressure coefficient, and failure proximity, a comprehensive risk index evaluation model was constructed, and the analytic hierarchy process was used to determine the weights of each indicator. Second, numerical simulations of casing deformation under different stress differences and rock Young's modulus conditions were carried out, and the influence of formation dip angle variation on casing deformation was analyzed. The results show that in the in situ stress reversal zones, multiple indicators overlap, indicating an extremely high risk of casing deformation, with stress difference and stress ratio being the main controlling factors. For the formation block in this study, when the stress difference exceeds 15 MPa, the radial displacement of the casing increases significantly. In addition, when the formation dip angle exceeds 50°, casing deformation increases sharply, and the coupling effect of compression and shear significantly increases the risk of casing deformation. The above results have important guiding significance for casing deformation assessment in the target block.

Keywords: coalbed methane; in situ stress; numerical simulation; casing deformation; formation dip angle

Check for updates

Academic Editor: Kun Sang Lee

Received: 22 August 2026
Revised: 8 October 2026
Accepted: 9 October 2026
Published: 14 October 2026

Copyright: © 2026 by the authors. Licensee MDPI, Basel, Switzerland. This article is an open access article distributed under the terms and conditions of the Creative Commons Attribution (CC BY) license.

1. Introduction

Casing deformation in coal seams is a frequently encountered engineering challenge during the development of shale gas and coalbed methane. Especially in complex tectonic stress zones, casing damage directly affects wellbore integrity, fracturing effectiveness, and single-well productivity [1,2]. In recent years, researchers have conducted extensive theoretical analyses, experimental tests, and numerical simulations on in situ stress characteristics and casing mechanical response mechanisms, achieving a series of important advances.

In terms of coalbed in situ stress and casing deformation risk assessment, researchers generally agree that horizontal principal stress difference is the fundamental cause of

non-uniform loading on the casing, leading to subsequent deformation. Under strike-slip fault and reverse fault stress states, the horizontal principal stress exceeds the vertical principal stress, subjecting the casing to significant lateral compressive loads [3–5]. Based on statistical analyses of extensive measured in situ stress data, the distribution characteristics of in situ stress in different basins and strata have been preliminarily revealed, and casing deformation risk assessment methods based on parameters such as stress difference have been established [6,7]. Studies show a significant positive correlation between casing deformation and stress difference; when the stress difference exceeds a certain range, the probability of casing deformation increases substantially. Regarding in situ stress testing, hydraulic fracturing, acoustic emission, differential strain analysis, and well log inversion are the most commonly used technical approaches, among which hydraulic fracturing is considered an important method for coal-rock in situ stress measurement due to its relative simplicity and reliable results [8–10]. Based on these methods, researchers have systematically tested the in situ stress characteristics of coal seams with different coal ranks and structural positions, revealing an overall linear increasing trend of coalbed in situ stress with burial depth. However, due to the low strength and strong heterogeneity of coal seams themselves, their in situ stress distribution often exhibits greater dispersion and local anomalies compared to conventional sandstone layers [11,12]. Significant differences exist between coal seam in situ stress and the surrounding roof and floor strata, with stress release or stress concentration phenomena frequently occurring within the coal seam itself. These differences are important causes of casing deformation, wellbore instability, and asymmetric fracture propagation [13,14]. Some studies have further explored the relationship between in situ stress and coal-rock mechanical parameters, finding that formation mechanical parameters such as Young's modulus, Poisson's ratio, and compressive strength are closely related to the magnitude and state of in situ stress. Coal-rock intervals with low modulus and high Poisson's ratio often correspond to lower stress levels or local stress reversal [15–17]. However, existing research has mostly focused on the testing and description of in situ stress data, while studies on multi-parameter fusion evaluation of in situ stress and quantitative correlation with engineering risks remain relatively weak. There is a particular lack of comprehensive evaluation methods for casing deformation risk that consider in situ stress heterogeneity and local anomalies.

Regarding numerical simulation of casing deformation, the finite element method has been widely used to analyze casing mechanical response under different working conditions. By establishing casing-cement sheath-formation assembly models and setting different stress differences, rock mechanical parameters, cement sheath properties, and construction conditions, researchers have simulated the radial displacement, stress distribution, and plastic yield characteristics of casings [18,19]. Studies indicate that stress difference is a key factor controlling the degree of casing deformation, with casing radial displacement exhibiting a nonlinear increasing trend as stress difference increases. Rock Young's modulus also has a certain influence on casing deformation; low-stiffness formations provide weaker constraint on the casing, making it more susceptible to yield under non-uniform loads [20–22]. The integrity and mechanical properties of the cement sheath also affect load transfer efficiency. In recent years, some studies have begun to focus on the influence of geological factors such as formation dip angle on casing deformation. By rotating the coordinate system to simulate in situ stress redistribution under different dip angle conditions, it has been found that the shear stress component increases in high-dip formations, subjecting the casing to coupled compression and shear effects [23,24]. Nevertheless, existing numerical simulation studies have mostly concentrated on sensitivity analyses of stress difference and rock mechanical parameters. Systematic investigations of casing deformation mechanisms when the formation dip angle exceeds a certain threshold

remain relatively limited, and quantitative comparisons of casing deformation patterns under different dip angle conditions are lacking.

In summary, although existing research has achieved certain results in in situ stress evaluation and casing simulation, the following deficiencies remain. First, casing deformation risk assessment indicators are relatively dispersed, lacking comprehensive evaluation methods that integrate multiple indicators along with weight allocation mechanisms. Second, numerical simulation studies on the influence of formation dip angle on casing deformation are still insufficient, particularly lacking systematic parameter sensitivity analysis. To address the above issues, this paper constructs a comprehensive risk index evaluation method based on five indicators including stress difference, stress ratio, maximum shear stress, lateral pressure coefficient, and failure proximity. The analytic hierarchy process is used to determine the weights of each indicator. Numerical simulations of casing deformation are carried out under different stress differences, rock Young's modulus values, and formation dip angles, aiming to provide a theoretical basis for the prediction and prevention of coal seam casing deformation. This method mainly lies in comprehensively considering the stress distribution of the formation and the combined effects among formation stresses, thereby improving the reliability of the casing deformation risk analysis results.

2. Methods

2.1. Calculation Model for In Situ Stress and Rock Mechanical Parameters

Young's modulus and Poisson's ratio are the two most fundamental elastic parameters describing rock mechanical behavior. Their accuracy directly affects the reliability of in situ stress calculation, wellbore stability evaluation, and casing deformation risk prediction. Young's modulus refers to the ratio of stress to strain in rock under uniaxial compression conditions, characterizing the rock's ability to resist elastic deformation. The larger the Young's modulus value, the greater the rock strength, and the smaller the elastic strain generated under the same stress. Poisson's ratio refers to the ratio of lateral strain to axial strain in rock under uniaxial compression conditions, characterizing the degree of lateral expansion of the rock when subjected to stress. The larger the Poisson's ratio, the higher the proportion of vertical stress converted into horizontal directional stress, which directly affects the magnitude of in situ stress and the two-directional stress difference.

Based on acoustic travel time and density logging data, Young's modulus and Poisson's ratio of rock can be calculated. The compressional wave travel time is usually measured directly in well logging, from which the compressional wave velocity can be obtained. There exists a specific physical relationship between compressional wave velocity and shear wave velocity. Therefore, the shear wave velocity can be derived from the compressional wave velocity as follows:

$$V_p = \frac{1}{\Delta t_p} \tag{1}$$

$$V_s = (0.61 \sim 0.53) V_p \tag{2}$$

where Δt_p is the compressional wave travel time, V_p is the compressional wave velocity, and V_s is the shear wave velocity.

Based on the shear wave velocity, compressional wave velocity, and rock density, the dynamic Young's modulus and dynamic Poisson's ratio of the rock can be calculated as follows:

$$E_d = \rho {V_s}^2 \frac{\left(3{V_p}^2 - 4{V_s}^2\right)}{\left({V_p}^2 - {V_s}^2\right)} \tag{3}$$

$$\mu_d = \frac{\left(V_p{}^2 - 2V_s{}^2\right)}{2\left(V_p{}^2 - V_s{}^2\right)} \tag{4}$$

where ρ is the rock density, E_d is the dynamic Young's modulus, and μ_d is the dynamic Poisson's ratio.

Static Young's modulus and Poisson's ratio are key parameters for calculating in situ stress. After obtaining the dynamic Young's modulus and Poisson's ratio, the static Young's modulus and Poisson's ratio are derived through a dynamic-static conversion model as follows:

$$E_s = aE_d + n \tag{5}$$

$$\mu_s = b\mu_d + m \tag{6}$$

where E_s is the static Young's modulus, μ_s is the static Poisson's ratio, and a, b, n, m are constants which can be obtained through rock mechanical experiments. These constants were obtained in this study from some measured values within the study area, and are usually taken as the average of the values from four nearby wells.

Young's modulus and Poisson's ratio can evaluate the deformation strength of rock but cannot directly describe the stress state of rock in the formation. The overburden pressure, maximum horizontal principal stress, and minimum horizontal principal stress can effectively characterize the stress state of the formation. Overburden pressure refers to the total vertical pressure generated by the rock matrix and pore fluid in the formation above a certain depth. Based on point-by-point integration of density logging data, the overburden pressure can be calculated as follows:

$$\sigma_v^i = \frac{\rho_0 H_0 + \sum_i \rho_i dh_i}{H_0 + \sum_i dh_i} \tag{7}$$

$$\sigma_H = \left(\frac{\mu_s}{1-\mu_s} + \xi_1\right)(\sigma_v - \alpha P_p) + \alpha P_p \tag{8}$$

$$\sigma_h = \left(\frac{\mu_s}{1-\mu_s} + \xi_2\right)(\sigma_v - \alpha P_p) + \alpha P_p \tag{9}$$

where σ_v^i is the overburden pressure gradient, ρ_0 is the average density of the section without density logging data, ρ_i is the logging density data, H_0 is the length of the section without density logging data, dh_i is the formation thickness of the corresponding interval, σ_H is the maximum horizontal principal stress, σ_h is the minimum horizontal principal stress, σ_v is the overburden pressure, α is the effective stress coefficient, ξ_1 and ξ_2 are tectonic stress coefficients, and P_p is the formation pore pressure.

2.2. Formation Casing Deformation Risk Assessment Method Based on In Situ Stress

In situ stress is the fundamental mechanical factor controlling casing deformation in coalbed methane wells. Coal seams are typically characterized by well-developed cleats, low mechanical strength, and significant anisotropy. During drilling, fracturing, and drainage processes, the non-uniformity of in situ stress is transmitted to the casing wall through the casing-cement sheath-formation assembly, inducing deformation failures such as diameter reduction, ovalization, and shear misalignment. Therefore, quantitatively evaluating the influence of in-situ stress characteristics on casing deformation risk is a key step in preventing casing deformation, optimizing wellbore structure, and designing fracturing schemes. The horizontal principal stress difference, horizontal principal stress ratio, lateral pressure coefficient, maximum shear stress, and failure proximity can be used to measure the distribution of anisotropic stress in the formation, thereby elucidating the

risk of formation casing deformation. Among these indicators, the horizontal principal stress difference, horizontal principal stress ratio, lateral pressure coefficient, and maximum shear stress focus on characterizing the degree of non-uniformity and the magnitude relationship of the stress field, while failure proximity further incorporates material strength characteristics, enabling a more comprehensive assessment of the state of the formation or casing approaching failure. The stress difference and maximum shear stress directly reflect the intensity of non-uniform loading. The stress ratio and lateral pressure coefficient describe the type and directionality of the stress field. Failure proximity provides a quantitative criterion combined with material failure criteria. In practical applications, multiple indicators are typically used together to construct a comprehensive rating system for casing deformation risk, thereby identifying high-risk intervals and guiding the formulation of engineering prevention and control measures.

The difference between the maximum horizontal principal stress and the minimum horizontal principal stress (Equation (10)) is the most direct and commonly used indicator for evaluating casing deformation risk. The larger the difference, the stronger the non-uniformity of the horizontal stress field, and the greater the elliptical compressive load borne by the casing, making it more susceptible to diameter reduction deformation or collapse failure. In coalbed methane wells, a high stress difference is often the dominant factor controlling casing deformation. Particularly during fracturing operations, an excessively large stress difference can limit the propagation morphology of hydraulic fractures while exacerbating local stress concentration on the casing.

$$\Delta\sigma = \sigma_H - \sigma_h \tag{10}$$

$$k = \frac{\sigma_H}{\sigma_h} \tag{11}$$

The stress ratio refers to the ratio of the maximum horizontal principal stress to the minimum horizontal principal stress (Equation (11)), reflecting the degree of anisotropy of the horizontal stress field. The closer the stress ratio is to 1, the more uniform the stress field, the more symmetric the loading on the casing, and the lower the risk of deformation. The larger the stress ratio, the more pronounced the non-uniform external extrusion load on the casing, making it prone to ovalization deformation or even rupture. This indicator correlates with the stress difference, but its dimensionless nature makes it more convenient for comparative analysis across different blocks and different depths.

$$\lambda = \frac{\sigma_H + \sigma_h}{2\sigma_v} \tag{12}$$

$$\tau_{max} = max\left(\frac{\sigma_H - \sigma_h}{2}, \frac{|\sigma_H - \sigma_v|}{2}, \frac{|\sigma_v - \sigma_h|}{2}\right) \tag{13}$$

The lateral pressure coefficient is the ratio of the sum of the maximum horizontal principal stress and the minimum horizontal principal stress to twice the vertical principal stress (Equation (12)), characterizing the magnitude of horizontal stress relative to vertical stress and reflecting the type of crustal stress field.

The maximum shear stress is an important mechanical indicator for determining whether the rock or the material surrounding the casing has reached yield or failure (Equation (13)). In the casing-cement sheath-formation assembly, the magnitude of the maximum shear stress directly reflects the intensity of asymmetric loading on the casing. When the maximum shear stress exceeds the shear strength of the material, shear failure will occur. For casing deformation risk assessment, the higher the maximum shear stress, the greater the possibility of shear misalignment or diameter reduction deformation of the casing.

Failure proximity is a comprehensive parameter for evaluating the degree to which the formation or the rock surrounding the casing approaches a failure state (Equation (14)), defined as the ratio of the distance from the current stress state to the failure boundary to the distance from the failure boundary to a certain reference point. This indicator integrates principal stress magnitude, stress difference, and material strength characteristics, and can quantitatively characterize the degree of plastic yield of the formation around the casing.

Based on the above evaluation indicators, this study proposes a comprehensive risk index (Equation (15)) for comprehensively assessing the risk of formation casing deformation. This index introduces weight coefficients, through which multiple indicators are integrated.

$$FI = \frac{\tau_{max}}{\tau_{lim}} \tag{14}$$

$$CRI = a{\cdot}\Delta\sigma' + b{\cdot}k' + c{\cdot}\lambda' + d{\cdot}\tau_{max}{}' + \mathrm{e}{\cdot}FI', \quad a+b+c+d+e=1 \tag{15}$$

where τ_{max} is the maximum shear stress borne by the rock under the current stress state, τ_{lim} is the ultimate shear stress that the rock can withstand, a, b, c, d, e are weight coefficients determined by comparing individual indicator analyses with actual results, and $\Delta\sigma'$, k', λ', $\tau_{max}{}'$, FI' are the normalized values of stress difference, stress ratio, lateral pressure coefficient, maximum shear stress, and failure proximity, respectively.

2.3. Numerical Simulation Model for Coal Seam Casing Deformation

Casing deformation is the result of the synergistic interaction among the formation, cement sheath, and casing (Figure 1). During coalbed methane extraction, engineering activities such as drilling, fracturing, and drainage induce redistribution of the in situ stress field. The non-uniform in situ stress is transmitted through the formation to the cement sheath and then from the cement sheath to the casing wall, leading to stress concentration and even plastic yield deformation of the casing. Therefore, establishing a mechanical model comprising the three-layer structure of formation, cement sheath, and casing, along with selecting appropriate yield criteria based on the mechanical characteristics of different materials, is the core approach for quantitatively evaluating casing deformation risk. The casing is made of ductile metallic material, and the Von Mises yield criterion is adopted. This criterion considers the influence of the intermediate principal stress and is suitable for describing the yield behavior of steel under complex stress states. The formation and cement sheath are geomaterials characterized by compression-shear failure and sensitivity to hydrostatic pressure. The Drucker-Prager yield criterion is adopted. This criterion can reflect the strength enhancement of geomaterials under high pressure and is more suitable than the Von Mises criterion as a failure criterion for coal rock and cement sheath. The model comprehensively considers the influence of in situ stress non-uniformity and differences in formation mechanical parameters on casing loading, enabling the simulation of casing deformation processes under different working conditions.

The Von Mises yield criterion is based on the distortion energy theory, which states that a material enters a plastic state when the equivalent stress reaches the uniaxial tensile yield strength of the material. Its core expression is as follows:

$$\sigma_{vm} = \sqrt{\frac{1}{2}\left[(\sigma_1-\sigma_2)^2 + (\sigma_2-\sigma_3)^2 + (\sigma_1-\sigma_3)^2\right]} \le \sigma_y \tag{16}$$

where σ_{vm} is the Von Mises equivalent stress, σ_1, σ_2, and σ_3 are the three principal stresses ($\sigma_1 > \sigma_2 > \sigma_3$), and σ_y is the yield strength of the casing material. When $\sigma_{vm} > \sigma_y$, the casing enters a yield state.

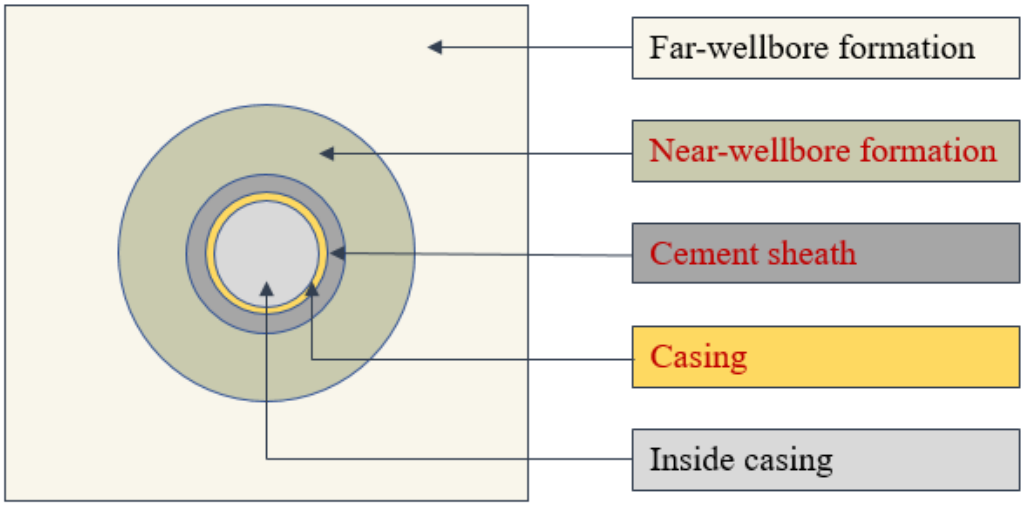


Figure 1. Geometric model of casing deformation.

The Drucker-Prager yield criterion is a smooth approximation of the Mohr-Coulomb criterion, overcoming the numerical difficulties of the latter at the corners while retaining the essential characteristics of pressure sensitivity of geomaterials. The yield function is expressed as follows:

$$\sqrt{J_2} + \alpha I_1 = K_f \tag{17}$$

$$I_1 = \sigma_1 + \sigma_2 + \sigma_3 \tag{18}$$

$$J_2 = \frac{1}{6}[(\sigma_1 - \sigma_2)^2 + (\sigma_2 - \sigma_3)^2 + (\sigma_1 - \sigma_3)^2] \tag{19}$$

$$\alpha = \frac{\sqrt{3}sin\varphi}{3\sqrt{3} + sin^2\varphi} \tag{20}$$

$$K_f = \frac{\sqrt{3}cos\varphi}{3\sqrt{3} + sin^2\varphi}C \tag{21}$$

where J_2 is the second invariant of the deviatoric stress tensor, I_1 is the first invariant of the stress tensor, K_f and α are parameters related to material cohesion and internal friction angle, φ is the internal friction angle of the material, and C is the material cohesion.

The casing-cement sheath-formation assembly is simplified as an axisymmetric annular model under plane strain conditions. The model consists of, from inside to outside, the casing, cement sheath, and formation. The external load on the model is a non-uniform in situ stress field, which results from the combined action of the maximum horizontal principal stress and the minimum horizontal principal stress.

3. Results

3.1. In Situ Stress Prediction and Evaluation

Based on the coal seam burial depth range of 1000~1800 m in the study area, combined with logging data from 21 wells and regional in situ stress measurements, the overburden pressure, maximum horizontal principal stress, and minimum horizontal principal stress were calculated using an in situ stress model. To determine some constants in the calculation model, this study conducted a comparative analysis using partial measured data from 21 wells to ensure that the calculation results are accurate and reliable. Meanwhile, dynamic Young's modulus and dynamic Poisson's ratio were calculated from acoustic logging data, and static Young's modulus and Poisson's ratio were obtained through dynamic-static conversion.

In the depth range of 1000~1800 m, the overburden pressure generally ranges from 37 to 48 MPa, the maximum horizontal principal stress ranges from 23 to 44 MPa, and the minimum horizontal principal stress ranges from 22 to 40 MPa (Figure 2). The overall magnitude relationship among the three stresses shows that the overburden pressure is greater than both the maximum and minimum horizontal principal stresses. Near a depth of 1270 m, a local reversal phenomenon occurs where the overburden pressure falls below the horizontal principal stresses, indicating possible stress unloading due to well-developed cleats, abnormal high pressure, or coalbed methane enrichment at this depth interval. Overall, the three curves exhibit an increasing trend with depth, and their fluctuation patterns show a certain correlation, reflecting the combined influence of formation heterogeneity on multiple stress components.

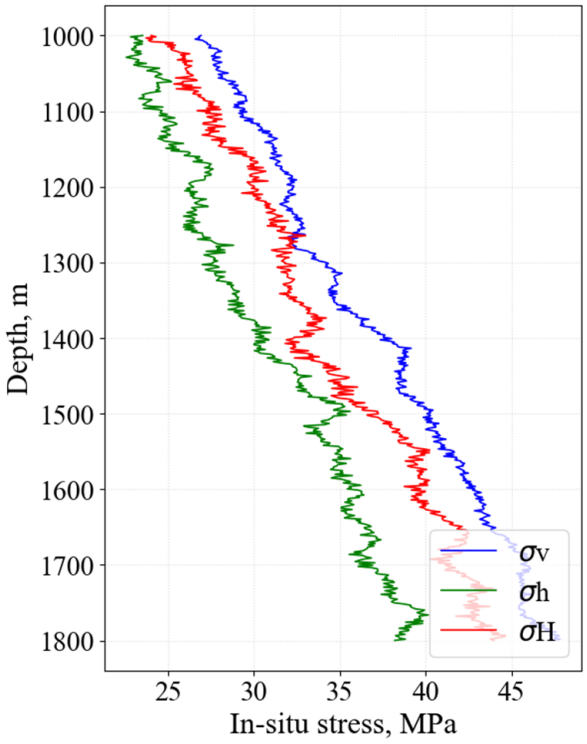


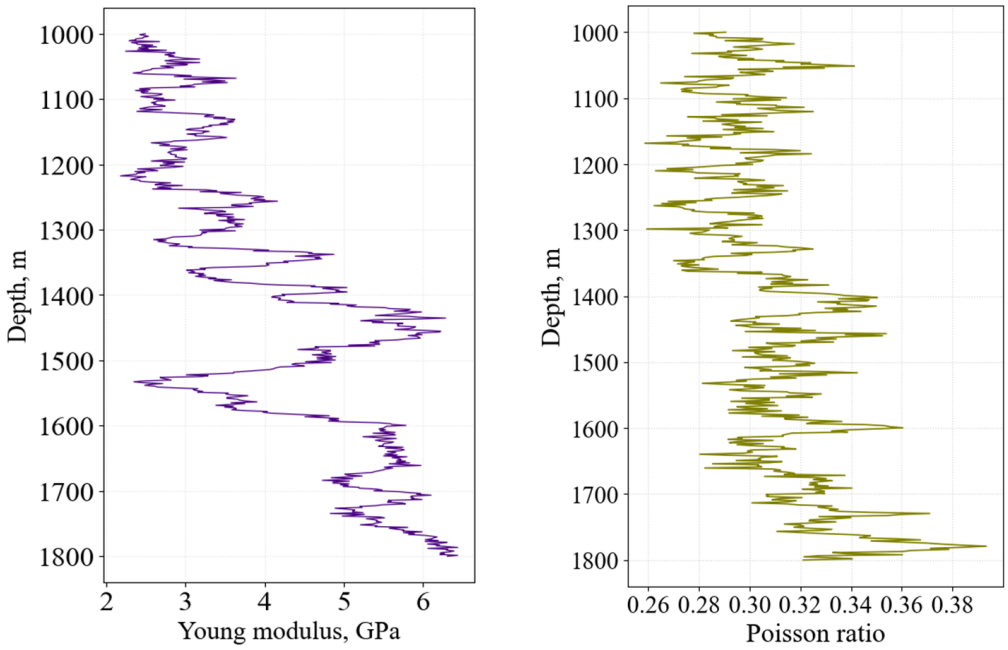
Figure 2. In situ stress calculation results of Well A.

Based on acoustic logging data, the static Young's modulus in the coal seam within the depth range of 1000~1800 m in the study area generally ranges from 2.1 to 6.6 GPa, showing an increasing trend with burial depth, which reflects the enhancement of compaction. A significant low-value depression occurs near 1540 m, corresponding to the development of thin coal seams, indicating that the coal rock has weak rigidity and is prone to compressive deformation. Static Poisson's ratio generally ranges from 0.26 to 0.39, with relatively small variation with depth (Figure 3). The variation patterns of the above mechanical parameters are consistent with the lithological interpretation results, providing a reliable parameter basis for subsequent in situ stress calculation and fracturing design.

3.2. Formation Casing Deformation Risk Classification

To systematically evaluate the risk of casing deformation in coal seams within the study area, five evaluation indicators were selected and divided into three groups for comprehensive analysis. The first group consists of stress difference and maximum shear stress, primarily used to characterize the magnitude of shear loading generated by differences in horizontal principal stresses. The larger the stress difference and the higher the shear stress, the stronger the non-uniform radial load on the casing, and the higher the risk of

shear deformation. The second group consists of stress ratio and lateral pressure coefficient. The stress ratio is defined as the ratio of the maximum horizontal principal stress to the minimum horizontal principal stress, representing the anisotropy of the horizontal stress field. The lateral pressure coefficient is defined as the ratio of horizontal stress to vertical stress, reflecting the relative relationship between horizontal and vertical stresses as well as the regional tectonic stress environment. The third group is failure proximity, which is based on the Drucker-Prager criterion and comprehensively reflects the degree to which the current stress state of the coal rock unit approaches the yield surface. It can be directly used to determine whether plastic yield of coal rock around the casing occurs and the risk of casing squeezing. Based on the above three groups of indicators, the casing deformation risk within the depth range of 1000~1800 m was analyzed section by section, and the comprehensive risk index was used to assess the risk of formation casing deformation.



(**a**) Young's Modulus (**b**) Poisson's Ratio

Figure 3. Calculation results of static rock mechanics parameters for Well A.

The calculation results of stress difference show that within the depth range of 1000~1800 m in the study area, the stress difference generally ranges from 2 to 28 MPa, and the maximum shear stress ranges from 2 to 13 MPa (Figures 4 and 5). Overall, both stress difference and shear stress increase with well depth. The maximum values of stress difference and shear stress can reach 28 MPa (at a depth of 1621 m) and 13 MPa (at a depth of 1595 m), respectively. In this region, the rock is subjected to strong non-uniform loading, which easily leads to local high stress concentration on the casing wall and increases the risk of casing deformation. Corresponding to the aforementioned in situ stress reversal zones (1450 m~1650 m), the stress difference in these intervals is greater than 15 MPa, and the shear stress is greater than 10 MPa, indicating concentrated horizontal tectonic stress in this region and a significant increase in the non-uniform load on the casing. Comprehensive analysis suggests that the risk of casing deformation is relatively high in the above depth intervals, and it is recommended to enhance wellbore integrity monitoring during fracturing and production processes.

The calculation results of the stress ratio and lateral pressure coefficient indicate that within the depth range of 1000~1800 m in the study area, the stress ratio generally ranges from 1.0 to 2.9, and the lateral pressure coefficient generally ranges from 0.5 to

1.5 (Figures 6 and 7). Overall, both the stress ratio and lateral pressure coefficient tend to increase with well depth. The maximum stress ratio can reach 2.9 (at a depth of 1583 m), and the maximum lateral pressure coefficient can reach 2.5 (at a depth of 1620 m), indicating that the region is generally in a strike-slip to reverse fault stress state, where horizontal tectonic stress plays a dominant role, and the risk of transverse compressive deformation of the casing increases. Corresponding to the aforementioned in situ stress reversal zones (1450 m~1650 m), the stress ratio in this interval is greater than 1.8, and the lateral pressure coefficient is greater than 1.2. In some sections, the lateral pressure coefficient exceeds 1.3, indicating that the minimum horizontal principal stress has exceeded the overburden pressure, significantly enhancing the compressive load on the casing from the horizontal direction, and even a circumferential uniform pressure state occurs in local sections. Comprehensive analysis suggests that tectonic compression is strong in the above depth intervals, and the risk of casing deformation is relatively high.

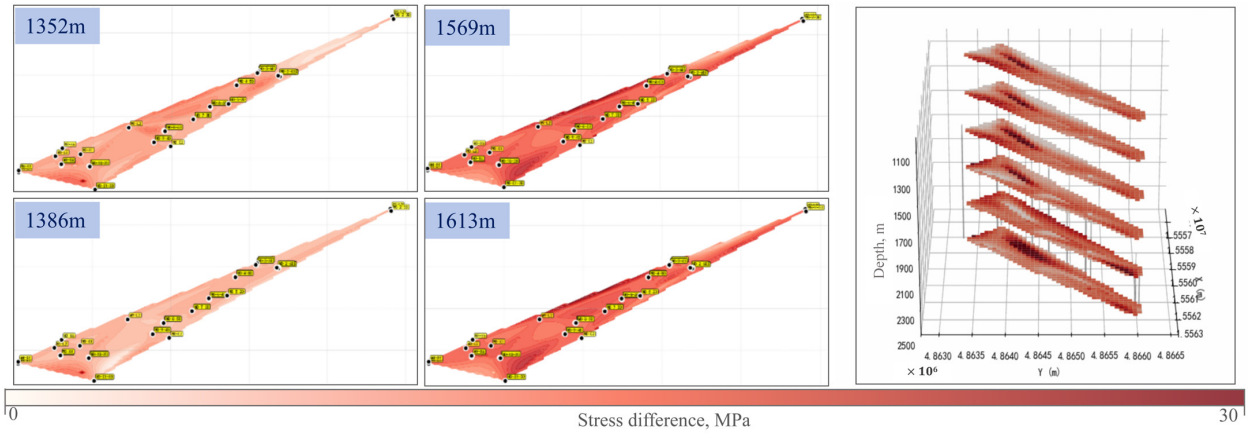


Figure 4. Stress difference analysis results.

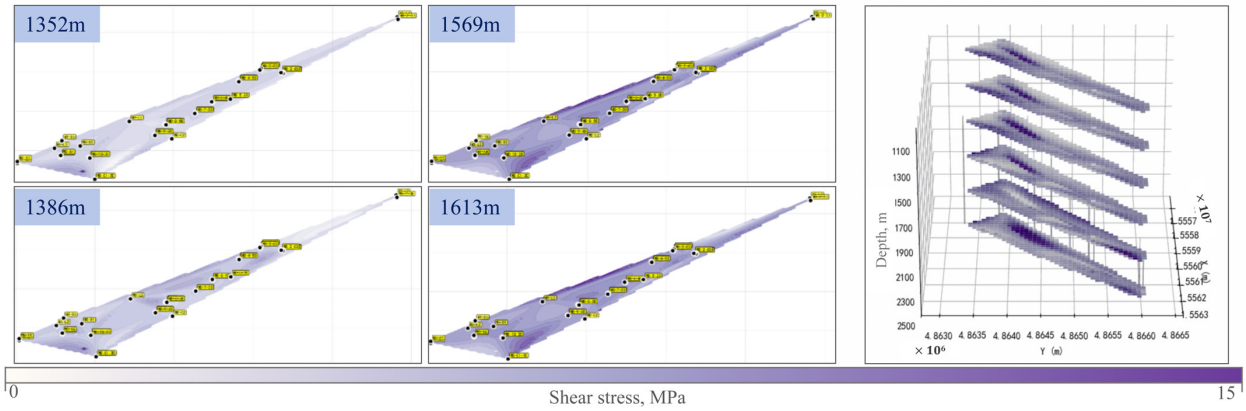


Figure 5. Shear stress analysis results.

The calculation results of failure proximity indicate that within the depth range of 1000~1800 m in the study area, the failure proximity generally ranges from 0.2 to 1.7 (Figure 8). Overall, the failure proximity exhibits a fluctuating upward trend with well depth. In the shallow section (1000~1200 m), the failure proximity is generally below 0.8, indicating a relatively low stress level in the coal rock at this interval, a greater distance from the yield surface, and relatively good stability of the rock mass around the casing. As burial depth increases, the failure proximity gradually increases, reflecting that the increase in in situ stress causes the coal rock to gradually approach a yield state. In the in situ stress reversal zones (1450~1650 m), the failure proximity exhibits a pronounced high-value zone, with a maximum value of up to 1.7 (at a depth of 1543 m), indicating that the coal rock in

this region is close to or already in a plastic yield state. The rock mass around the casing is prone to significant deformation or even failure, exerting strong non-uniform compression on the casing. In addition, in thin coal seam development sections, the failure proximity also shows locally elevated characteristics, which may be related to the low strength of the coal rock itself and its susceptibility to yield. Comprehensive analysis suggests that when the failure proximity exceeds 0.7, the risk of casing deformation increases significantly.

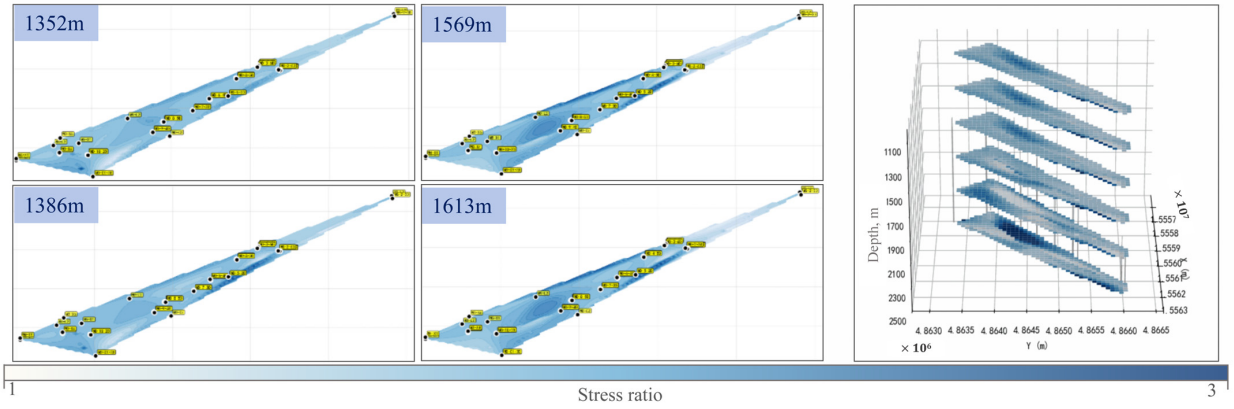


Figure 6. Stress ratio analysis results.

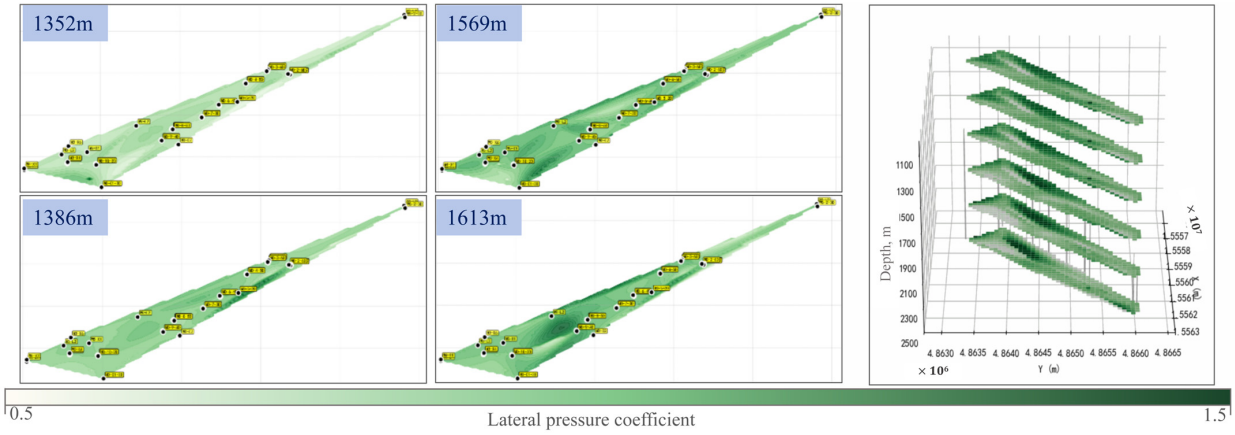


Figure 7. Lateral pressure coefficient analysis results.

The calculation results of the comprehensive risk index show that within the depth range of 1000~1800 m in the study area, the comprehensive risk index generally ranges from 0.2 to 1.6. In the well section from 1000 to 1300 m, the comprehensive risk index is generally low, with an average value of 0.4, indicating a low risk of casing deformation (Figure 9). In the in situ stress reversal zones (1450~1650 m), the average value of the comprehensive risk index reaches 0.8, with a maximum value of 1.6, indicating an extremely high risk of casing deformation.

According to the calculation results of the comprehensive risk index, combined with the actual casing deformation statistics within the study block, the casing deformation risk of coal seams in the study area is divided into three categories: low risk, medium risk, and high risk. For the formation block in this study, when CRI $\leq$ 0.6 (this threshold is only applicable to the block in this study and is not universally applicable to other areas), the formation casing deformation risk is low; when 0.6 $<$ CRI $\leq$ 1.0, the formation casing deformation risk is medium; when 1.0 $<$ CRI, the formation casing deformation risk is high (Figure 10). Within the study area, the high-risk zone for casing deformation accounts for 9.9%, the medium-risk zone accounts for 19.3%, and 70.8% of the area is classified as low-risk zone (Figure 11). The high-risk zones are mainly concentrated in areas with

large stress differences. Within the high-risk well sections, the high-risk zones for casing deformation mainly include three regions: A, B, and C. Casing deformation prevention and control should be emphasized in the above regions during construction (Figure 10).

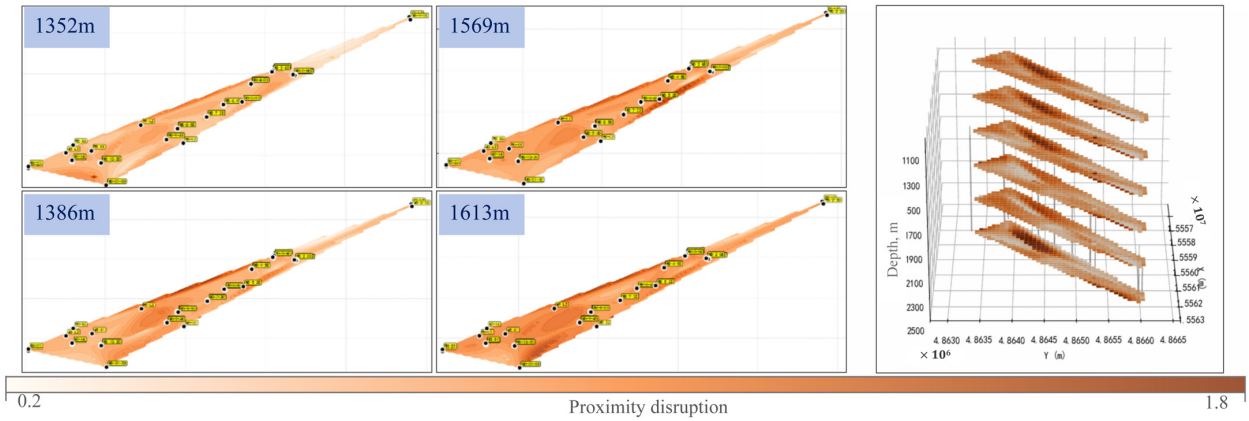


Figure 8. Failure proximity analysis results.

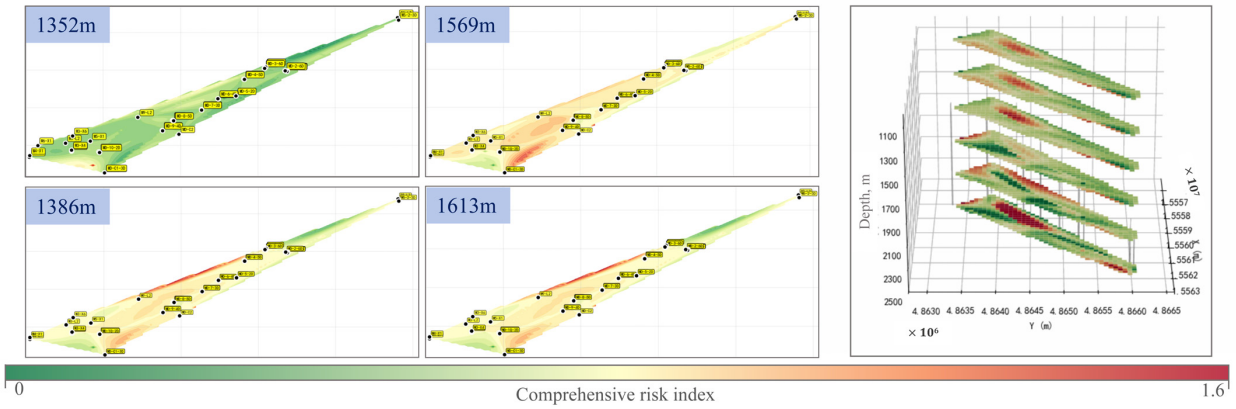


Figure 9. Comprehensive risk index analysis results.

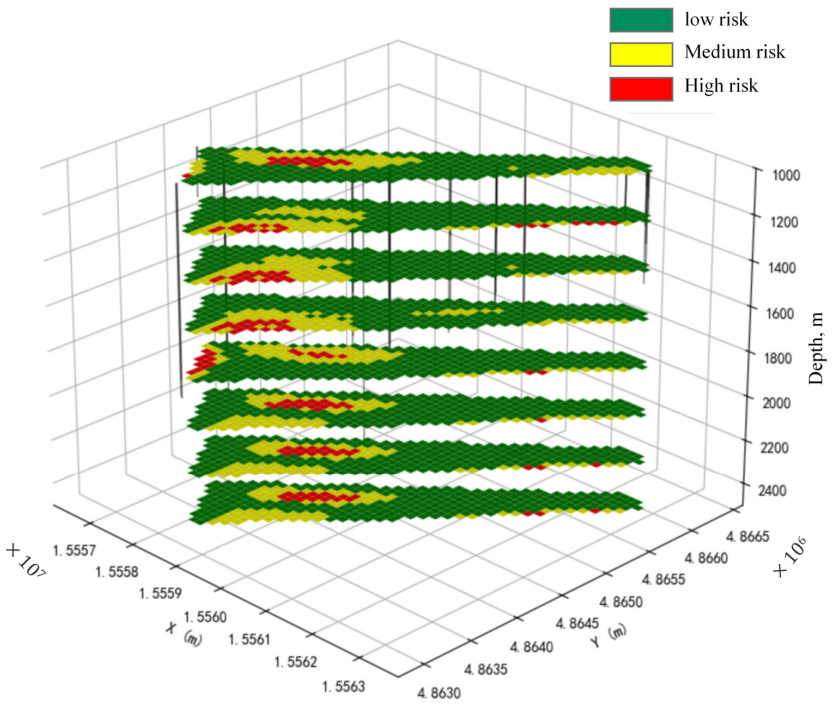


Figure 10. Identification of casing deformation risk zones.

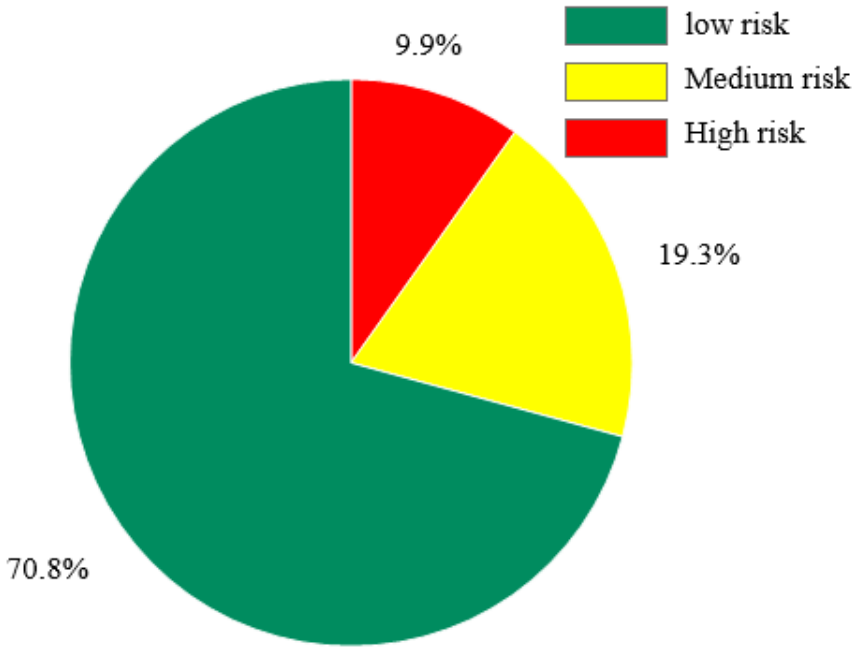


Figure 11. Statistics of casing deformation risk zones.

3.3. Numerical Simulation of Casing Deformation

To quantitatively evaluate the influence of stress difference on casing deformation, four horizontal stress difference conditions of 5 MPa, 10 MPa, 15 MPa and 20 MPa were set up respectively, and numerical simulation of casing deformation was carried out to obtain the variation law of casing radial displacement with stress difference. The simulation results show that when the stress difference is 5 MPa, the maximum radial displacement of the casing is 0.3 mm, and the casing basically remains in an elastic state with negligible deformation. When the stress difference increases to 10 MPa, the maximum radial displacement increases to 4.2 mm, but plastic yield has not yet occurred. When the stress difference reaches 15 MPa, the maximum radial displacement significantly increases to 11.3 mm, the casing locally enters a plastic state with obvious ovalization, and wellbore integrity is threatened. When the stress difference further increases to 20 MPa, the maximum radial displacement reaches 21.7 mm, and the casing undergoes severe collapse deformation with local instability (Figure 12). Comprehensive analysis indicates that when the stress difference exceeds 15 MPa, the risk of casing deformation increases significantly, which is consistent with the measured results of stress difference greater than 15 MPa in the aforementioned in situ stress reversal zones (1450~1650 m), verifying the conclusion that the casing deformation risk in this well section is extremely high.

To evaluate the influence of rock stiffness on casing deformation, four Young's modulus conditions of 2.5 GPa, 3.5 GPa, 4.5 GPa and 5.5 GPa were set up respectively, and numerical simulation of casing deformation was carried out under the same stress difference (10 MPa). The simulation results show that the influence of Young's modulus on the radial displacement of the casing is smaller than that of stress difference, but the variation pattern is clear. When the Young's modulus is 2.5 GPa, the maximum radial displacement of the casing is 19.1 mm, with the most significant deformation, indicating that low-stiffness rock has a weaker constraint capacity on the casing, and non-uniform loads are more likely to cause casing yield. When the Young's modulus increases to 3.5 GPa, the maximum radial displacement decreases to 14.8 mm; when it increases to 4.5 GPa, it further decreases to 12.6 mm; when the Young's modulus reaches 5.5 GPa (hard rock, corresponding to tight sandstone), the maximum radial displacement is 8.9 mm, and the degree of casing

deformation is significantly weakened (Figure 13). Comprehensive analysis indicates that the lower the rock Young's modulus, the more prone the casing is to deformation, meaning that the casing deformation risk in coal seam sections is higher than that in surrounding rock sections, which is consistent with the previous conclusion that the failure proximity increases in thin coal seam development areas.

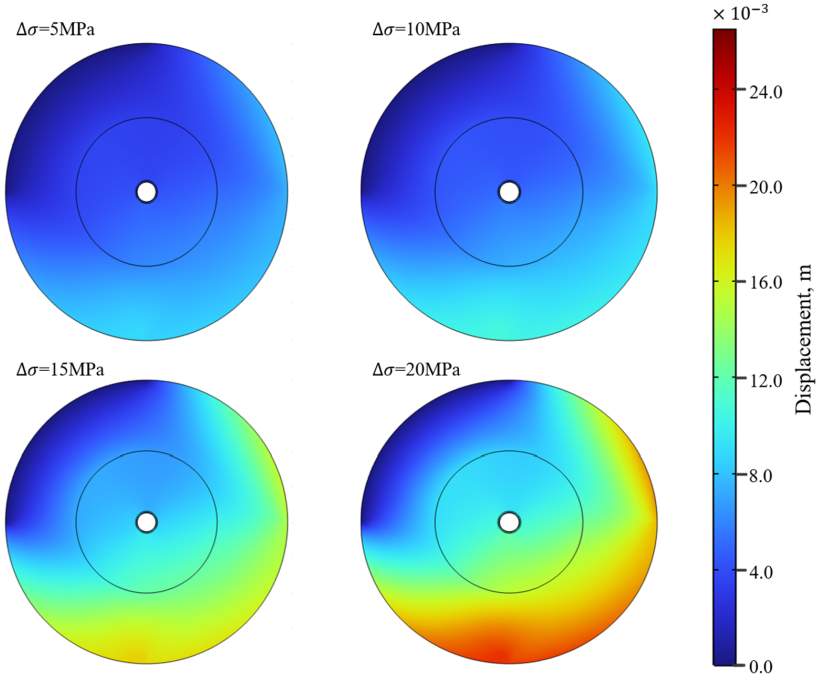


Figure 12. Simulation of casing deformation under different stress differences.

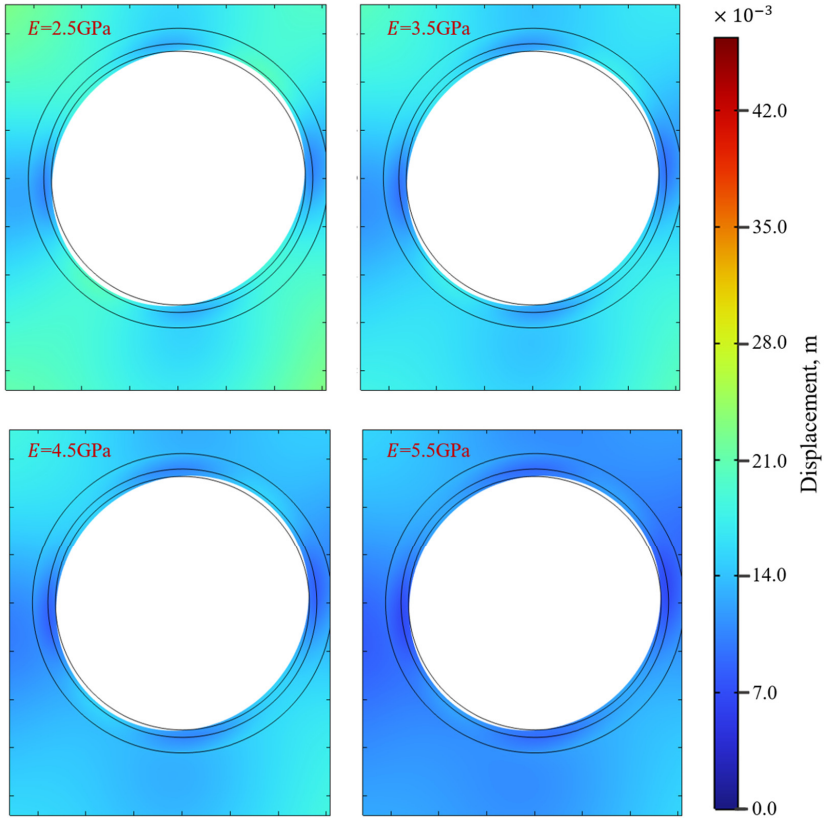


Figure 13. Simulation of casing deformation under different Young's modulus conditions.

4. Discussion

4.1. Influence of Different In Situ Stress Evaluation Methods on Casing Deformation Risk Classification

The comprehensive risk index method for formation casing deformation risk assessment is composed of five indicators: stress difference, stress ratio, maximum shear stress, lateral pressure coefficient, and failure proximity. Each indicator has a different weight in the evaluation system, reflecting the varying degrees of contribution of different mechanical factors to casing deformation risk. The analytic hierarchy process was used to determine the weights of each indicator. By constructing a judgment matrix and calculating the consistency ratio, the rationality of the weight allocation were ensured. The calculation results show that stress difference and stress ratio have the largest weights, being 0.38 and 0.29 respectively, together accounting for 67%, exceeding two-thirds of the total weight, indicating that horizontal principal stress difference and tectonic stress environment are the dominant factors controlling casing deformation risk. Among them, stress difference directly reflects the intensity of non-uniform loading in the horizontal direction, with the highest weight of 0.38, making it the core indicator for casing deformation risk assessment. The stress ratio, defined as the ratio of the maximum horizontal principal stress to the minimum horizontal principal stress, has a weight of 0.29 and is used to characterize the dominance of tectonic stress relative to vertical stress. Together, these two constitute the main control indicator system for casing deformation risk. The weights of maximum shear stress, failure proximity, and lateral pressure coefficient are 0.14, 0.11, and 0.08 respectively, together accounting for approximately 33%, serving as auxiliary indicators for the refinement and correction of formation casing deformation risk assessment (Figure 14). Among them, maximum shear stress reflects the absolute value of shear load, failure proximity comprehensively determines whether the coal rock is approaching a yield state, and the lateral pressure coefficient, defined as the ratio of the sum of the maximum and minimum horizontal principal stresses to the vertical stress, supplements structural information from the perspective of the ratio of the minimum horizontal principal stress to the vertical stress. The above weight allocation scheme indicates that casing deformation risk assessment should take stress difference and stress ratio as the core, supplemented by shear stress, failure proximity, and lateral pressure coefficient for local correction, thereby achieving a comprehensive and quantitative assessment of coal seam casing deformation risk.

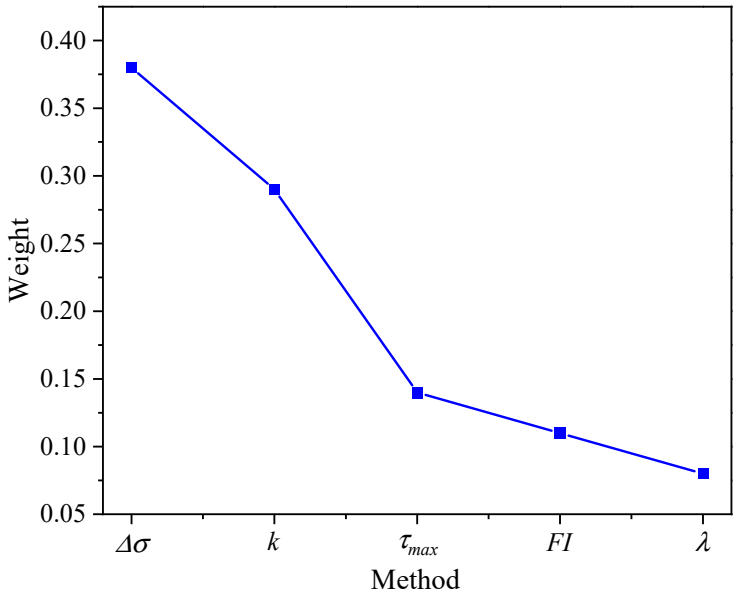
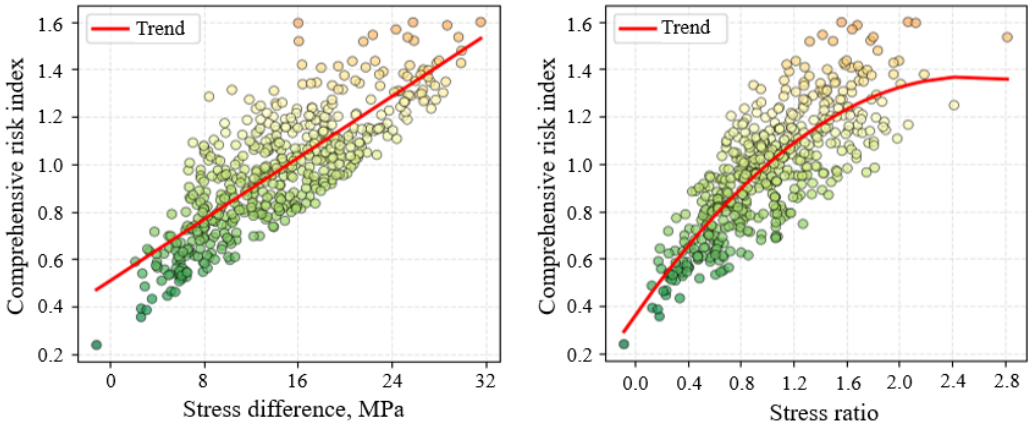


Figure 14. Weight coefficients of different evaluation indicators.

The stress difference and the comprehensive risk index basically show a linear positive correlation. The larger the stress difference, the higher the comprehensive risk index, indicating that the difference in horizontal principal stresses has a direct and nearly linear controlling effect on casing deformation risk. The stress ratio also shows a positive correlation with the comprehensive risk index, but with nonlinear characteristics. When the stress ratio is low, the comprehensive risk index increases slowly. After exceeding a certain threshold, the comprehensive risk index accelerates its rise. When the stress ratio reaches a relatively high level, the comprehensive risk index tends to level off (Figure 15). This nonlinear characteristic indicates that there is a threshold interval for the stress ratio. Below this interval, tectonic action is weak and casing deformation risk is controllable. After exceeding the threshold, tectonic compression is significantly enhanced and casing deformation risk rises rapidly, eventually entering a high-risk plateau. The above observations verify the rationality of stress difference and stress ratio as the main controlling indicators for casing deformation risk.



(**a**) Stress difference (**b**) Stress ratio

Figure 15. Relationship between stress difference, stress ratio and comprehensive risk index.

4.2. Influence of Formation Dip Angle on Casing Deformation

To investigate the influence of formation dip angle on casing deformation, this study simulates the distribution characteristics of in situ stress under different dip angle conditions by rotating the coordinate system. First, an initial in situ stress field is established in the coordinate system of horizontal layered strata, where the vertical principal stress and horizontal principal stresses are orthogonal to each other. When the formation has a dip angle, the initial in situ stress field is rotated to a new coordinate system parallel to the formation plane using a coordinate transformation matrix, i.e., rotating a specific angle around a certain horizontal axis, and this angle is the formation dip angle (Figure 16). After rotation, the original vertical principal stress and horizontal principal stresses are decomposed again in the new coordinate system, generating new normal stress components and shear stress components that act on the casing and surrounding rock mass. As the formation dip angle increases, the shear component gradually strengthens, and the non-uniform load pattern on the casing changes from primarily horizontal compression to a coupling of compression and shear. By setting up multiple sets of dip angle conditions and comparatively analyzing the casing radial displacement and stress distribution characteristics under different dip angles, the influence law of formation dip angle on casing deformation risk can be quantitatively evaluated.

To investigate the influence of formation dip angle on casing deformation, the casing radial displacement was simulated under four formation dip angle conditions: 30°, 40°, 50°, and 60°. The simulation results show that as the formation dip angle increases, the

maximum casing deformation exhibits an accelerating growth trend. When the formation dip angle is 30°, the maximum deformation is 21 mm; when increased to 40°, the maximum deformation is 24 mm, a relatively small increase; when the formation dip angle reaches 50°, the maximum deformation significantly jumps to 51 mm, more than double that of the 40° condition; when the dip angle further increases to 60°, the maximum deformation reaches 63 mm, and the casing undergoes severe collapse deformation (Figures 17 and 18). The above results indicate that when the formation dip angle is less than 40°, the degree of casing deformation is relatively controllable; when the dip angle exceeds 50°, the deformation increases sharply, and the casing deformation risk significantly rises. Analysis suggests that under high dip angle conditions, the shear stress component generated by coordinate rotation significantly enhances, and the casing transitions from primarily horizontal compression to a coupled compression-shear effect, leading to changes in the non-uniform load pattern and intensified local stress concentration. It is recommended to optimize casing selection and adopt targeted anti-deformation measures in well sections where the formation dip angle exceeds 50°.

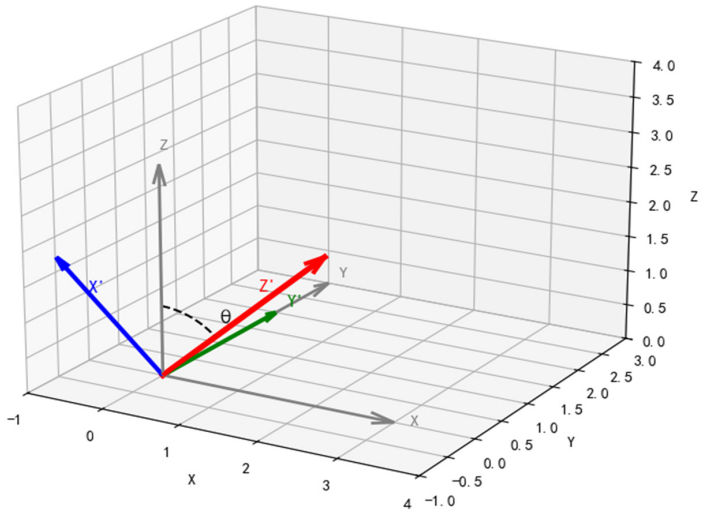


Figure 16. Simulation of formation dip angle variation by rotating the coordinate system.

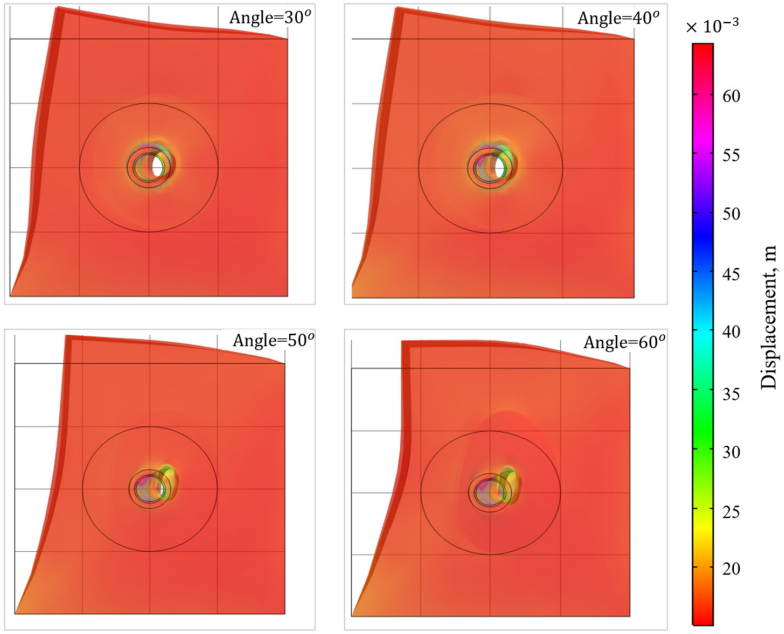


Figure 17. Simulation examples of casing deformation under different formation dip angle.

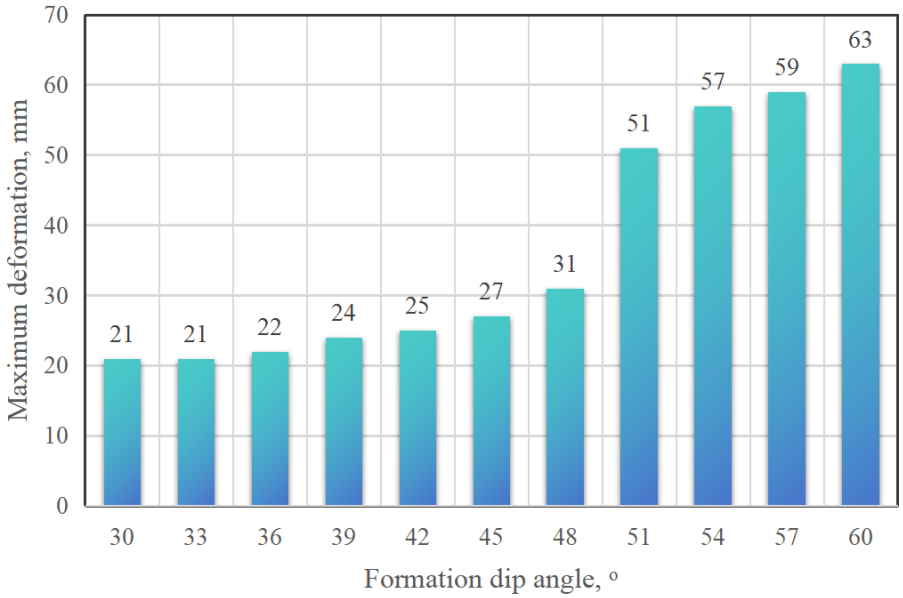


Figure 18. Relationship between formation dip angle and casing deformation.

5. Conclusions

This study takes the risk of coal seam casing deformation as the research object, comprehensively employing methods such as in situ stress evaluation, numerical simulation, and parameter sensitivity analysis to systematically carry out in situ stress characteristic analysis, casing deformation simulation under different stress difference and Young's modulus conditions, and investigation of the influence law of formation dip angle. The following main conclusions are drawn. The conclusions below are all specific to the study area and study conditions of this research, and are not universal results applicable to all studies:

(1) The comprehensive risk index evaluation results based on five indicators, namely stress difference, stress ratio, maximum shear stress, lateral pressure coefficient, and failure proximity, show that multiple indicators overlap in the in situ stress reversal zones, with the comprehensive risk index reaching its maximum value, indicating an extremely high risk of casing deformation. Among these, stress difference and stress ratio are the dominant controlling factors, with weights of 0.38 and 0.29, respectively. Both show a positive correlation with the comprehensive risk index, with stress difference exhibiting a linear relationship and stress ratio exhibiting a nonlinear characteristic.

(2) The numerical simulation results of casing deformation indicate that stress difference is a key factor controlling casing radial displacement. For the formation area in this study, when the stress difference exceeds 15 MPa, the risk of casing deformation increases significantly. Rock Young's modulus has a relatively smaller influence on casing deformation, with lower modulus corresponding to larger displacement, reflecting that soft rock provides weak constraint and is more prone to deformation.

(3) Formation dip angle has a significant influence on casing deformation. For the formation area in this study, when the formation dip angle exceeds 50°, the maximum casing deformation sharply jumps from 24 mm to 51 mm, reaching 63 mm at a dip angle of 60°, indicating that the coupling effect of compression and shear intensifies under high dip angle conditions, leading to a significant increase in casing deformation risk.

This study mainly aims to provide a new method for studying casing deformation. The quantitative conclusions obtained in this study are only applicable to the study block, and for new study areas, testing and verification should be carried out according to the method proposed in this study.

Author Contributions: Conceptualization, F.Z. and L.F.; Methodology, Y.H. and B.X.; Software, Y.B. and Y.F.; Validation, F.Z., B.X. and Y.H.; Formal analysis, B.X.; Data curation, Y.F. and Y.B.; Visualization, Y.F.; Supervisio, L.F.; Writing—review and editing, F.Z., L.F., Y.H. and Y.B. All authors have read and agreed to the published version of the manuscript.

Funding: This work was supported by China Offshore Oil Group Co., Ltd. Science and Technology Project 'Key Technology Research and Application of Drilling and Completion in Xinjiang High Steep Coal Seam' (KJZH-2025-2306).

Institutional Review Board Statement: Not applicable.

Informed Consent Statement: Not applicable.

Data Availability Statement: The simulated dataset and source code presented in this study are available on request from the corresponding author.

Conflicts of Interest: Author Lei Feng and Fei Zhang were employed by the company China United Coalbed Methane Corp., Ltd. Author Yuan Hao was employed by the company Wulumuqi Guosheng Huidong New Energy Co., Ltd. The remaining authors declare that the research was conducted in the absence of any commercial or financial relationships that could be construed as a potential conflict of interest.

References

1. Wang, Z.; Yang, X.; Wang, G.; Gong, H. Study on Instability Characteristics of the Directional Borehole on the Coal-Seam Roof: A Case Study of the Tingnan Coal Mine. *Processes* **2023**, *11*, 1675. [CrossRef]
2. Liu, F.; Ge, G.H.; Gong, P. Simulation on the deformation of surrounding rock in fully mechanized top coal caving face in thick loose seam. *Therm. Sci.* **2025**, *29*, 1123–1129. [CrossRef]
3. Rao, Z.; Du, Q.; Xiang, C.; Han, Z.; Liang, Y. A Numerical Simulation Investigation on the Distribution Characteristics of Coal Seam In Situ Stress Under the Influence of Normal Fault. *Processes* **2025**, *13*, 538. [CrossRef]
4. Yang, S.; Wang, J.; Chen, J.; Liang, B.; Ren, L.; Xin, T. Study on the response mechanism characteristics of fault activation under the mining effect of thick coal seam. *J. Appl. Geophys.* **2025**, *243*, 105954. [CrossRef]
5. Wu, Z.; Zhong, D.; Wang, L.; Bi, L. Coal Seam Geological Implicit Modeling with Fault Networks and Kinematic Parameters. *Math. Geosci.* **2025**, *58*, 1561–1582. [CrossRef]
6. Wang, G.; Wang, S.; Liu, Y.; Huang, Q.; Li, S.; Xie, S.; Zheng, J.; Fan, J. Influences of clean fracturing fluid viscosity and horizontal in-situ stress difference on hydraulic fracture propagation and morphology in coal seam. *Int. J. Coal Sci. Technol.* **2024**, *11*, 38. [CrossRef]
7. Zhao, K.; Huang, P.; He, Y.; Cui, L.; Liu, P.; Feng, Y.; Sun, X.; Cao, S. Effect of Geostress Variation on Hydraulic Fracturing Behavior and Stress Redistribution in Coal Seam Roofs. *Processes* **2025**, *13*, 1732. [CrossRef]
8. Ran, Q.; Liang, Y.; Ye, C.; Ning, Y.; Ma, T.; Kong, F. Failure analysis of overlying strata during inclined coal seam mining: Insights from acoustic emission monitoring. *Eng. Fail. Anal.* **2025**, *182*, 110023. [CrossRef]
9. Duan, M.; Lu, M.; Ban, R.; Cheng, A.; Yang, K.; Tang, J.; Guo, C. Study on the influence of coal thickness on the mechanics and acoustic emission characteristics of gas-bearing coal and rock mass. *Phys. Fluids* **2025**, *37*, 017151. [CrossRef]
10. Wang, C.; Liu, W.; He, M.; Niu, S.; Hou, J. Non-destructive evaluation of failure mechanisms in multilayered coal-rock specimens using acoustic emission characterisation. *Nondestruct. Test. Eval.* **2026**, *41*, 1630–1647. [CrossRef]
11. Feng, Y.L.; Wu, L.Y. Study on Distribution Law of Ground Stress in Main Coal Seam of Qinshui Coalfield. *Lithosphere* **2025**, *1*, 2024197. [CrossRef]
12. Kurlenya, M.V.; Lee, K.H.; Kazantsev, V.G.; Lee, E.H. Physical-Mathematical Model of Methane Flow in Nonstationary Stress Field in Coal Seam. *J. Min. Sci.* **2024**, *60*, 357–365. [CrossRef]
13. Wang, H.; Xie, L.; Li, Y.; Hao, Y.; Qi, X. Study on the Formation and Evolution of Constant Stress Concentration Shell in Overburden Rock Strata During Coal Seam Mining. *Rock Mech. Rock Eng.* **2025**, *58*, 9363–9390. [CrossRef]
14. Chen, Y.; Chu, T.; Chen, X.; Jiang, B.; Chen, P.; Cao, J.; He, N. Spatiotemporal evolutions of gas pressures in coal seam during gas extraction under mining disturbance. *Sci. Rep.* **2024**, *14*, 30253. [CrossRef] [PubMed]
15. Lu, J.; Meng, X.; Wang, Y.; Yang, Z. Prediction of coal seam details and mining safety using multicomponent seismic data: A case history from China. *Geophysics* **2017**, *81*, 149–165. [CrossRef]
16. Zheng, C.; Jiang, B.; Yuan, L.; Kizil, M.; Xue, S.; Han, B.; Tang, M.; Chen, Z. Effects of heterogenous interburden Young's modulus on permeability characteristics of underlying relieved coal seam: Implementation of damage-based permeability model. *J. Nat. Gas. Sci. Eng.* **2021**, *96*, 104317. [CrossRef]

17. Khan, M.; He, X.; Song, D.; Tian, X.; Li, Z.; Xue, Y.; Aslam, K.S. Extracting and Predicting Rock Mechanical Behavior Based on Microseismic Spatio-temporal Response in an Ultra-thick Coal Seam Mine. *Rock Mech. Rock Eng.* **2023**, *56*, 3725–3754. [CrossRef]
18. Chen, J.H.; Wang, T.; Zhou, Y.; Zhu, Y.; Wang, X. Failure modes of the surface venthole casing during longwall coal extraction: A case study. *Int. J. Coal Geol.* **2012**, *90*, 135–148. [CrossRef]
19. Li, Z.; Xu, G.; Zhang, Z.; Zhao, G. Hydraulic Fracturing Pressure Relief for Pillar Size Optimization in Ultra-Thick Coal Seam Longwall Panels: Design, Monitoring, and Field Verification. *Processes* **1975**, *13*, 2975.
20. Song, S.; Liu, X.; Tan, Y.; Li, X.; Yang, S.; Zhang, Y. Failure Characteristics and Evolution Law of Overburden Structure Under Repeated Mining of Close-Distance Coal Seam Group in Ningdong Mining Area. *Energy Sci. Eng.* **2025**, *13*, 5627–5644. [CrossRef]
21. Li, D.Q. A new technology for the drilling of long boreholes for gas drainage in a soft coal seam. *J. Pet. Sci. Eng.* **2016**, *137*, 107–112. [CrossRef]
22. Zhang, B.; Ran, X.; Wang, Y.; Zhang, F.; Liang, W.; Li, Z. Experimental study on mechanical properties of coal rocks in re-fracturing. *Alex. Eng. J.* **2021**, *60*, 3315–3325. [CrossRef]
23. Yao, Q.; Li, X.; Sun, B.; Ju, M.; Chen, T.; Zhou, J.; Liang, S.; Qu, Q. Numerical investigation of the effects of coal seam dip angle on coal wall stability. *Int. J. Rock Mech. Min. Sci.* **2017**, *100*, 298–309. [CrossRef]
24. Zhao, P.; Chang, Z.; Li, S.; Zhuo, R.; Jia, Y.; Shao, Q.; Lei, W. Study and application of the influence of inclination angle on the cross-fusion mechanism of high gas thick coal seam. *Int. J. Min. Sci. Technol.* **2025**, *35*, 69–85. [CrossRef]

Disclaimer/Publisher's Note: The statements, opinions and data contained in all publications are solely those of the individual author(s) and contributor(s) and not of MDPI and/or the editor(s). MDPI and/or the editor(s) disclaim responsibility for any injury to people or property resulting from any ideas, methods, instructions or products referred to in the content.